Dalton Transactions

Low-Temperature Synthesis of Superconducting Iron Selenide Using a Triphenylphosphine Flux

Journal:	*Dalton Transactions*
Manuscript ID	DT-ART-09-2019-003723
Article Type:	Paper
Date Submitted by the Author:	18-Sep-2019
Complete List of Authors:	Fallon, Jewels; Colorado State University, Martinolich, Andrew; California Institute of Technology, Division of Chemistry and Chemical Engineering Maughan, Annalise; NREL Gallington, Leighanne; Argonne National Laboratory, X-ray Science Division Neilson, James; Colorado State University, Chemistry

Journal Name

ARTICLE TYPE

Cite this: DOI: 00.0000/xxxxxxxxxx

Low-Temperature Synthesis of Superconducting Iron Selenide Using a Triphenylphosphine Flux†

M. Jewels Fallon,[a] Andrew J. Martinolich,[a] Annalise E. Maughan,[a] Leighanne C. Gallington,[b] and James R. Neilson[a]

Received Date
Accepted Date

DOI: 00.0000/xxxxxxxxxx

Many functional materials have relatively low decomposition temperatures (T $\leq$ 400 °C), which makes their synthesis challenging using conventional high-temperature solid-state chemistry. Therefore, non-conventional techniques such as metathesis, hydrothermal, and solution chemistry are often employed to access low-temperature phases; the discovery of new chemistries is needed to expand access to these phases. This contribution discusses the use of triphenylphosphine (PPh_3) as a molten flux to synthesize superconducting iron selenide ($Fe_{1+\delta}Se$) at low temperature (T = 325 °C). Powder X-ray diffraction and magnetism measurements confirm the successful formation of superconducting iron selenide while nuclear magnetic resonance spectroscopy and in situ X-ray diffraction show that the formation of superconducting FeSe at low temperatures is enabled by an adduct between the triphenylphosphine and selenium. Exploration of the Fe-Se-PPh_3 phase space indicate that the PPh_3-Se adduct effectively reduces the chemical potential of the selenium at high concentrations of triphenylphosphine. This contribution demonstrates that the use of a poorly-solvating yet reactive flux has the potential to enable the synthesis of new low temperature phases of solid materials.

Many important functional inorganic materials are only stable, or are only able to be synthesized, below temperatures that are typically required for traditional reactions.[1] Phases which are only stable below T $\sim$ 400 °C are often challenging to synthesize and require complex or non-traditional synthetic methodologies that may limit potential applications. For example, many metal chalcogenides are only accessible with more challenging techniques such as high pressure or multiple complex regrinding and reheating schedules.[2,3] The discovery of new synthetic methods to access materials phases with stability only at low temperatures is therefore paramount for advancing materials discovery and will enable more widespread use of materials that are otherwise challenging to synthesize.[1]

Flux synthesis is a synthetic technique in which a compound that is molten at the reaction temperature is used to promote diffusion and enable reactivity between solid phases at lower temperatures. Traditionally, flux synthesis involves metallic melts (Sn, Bi), metal chlorides (LiCl, KCl), or alkali chalcogenides (Na_xS_y) as the molten phases.[1,4] For example, the eutectic mixture of NaCl and KCl has been used to grow single crystals of FeSe at T = 850 °C.[5] This compliments solvothermal synthesis, in which solvents are heated past their normal boiling points by heating in a closed vessel designed to hold elevated pressures. A solvothermal approach using ammonium chloride and ethane-1,2-diol has been used to prepare FeSe powders from elemental precursours at T = 200 °C relative to the salt flux or reaction from the elements.[6] These methods are all used to promote reactivity by aiding in mass transport at relatively low temperatures.

In this contribution, we illustrate the use of a hybrid approach: an organic flux that enables the reaction between iron and selenium at low temperatures. These molecules have long been used to control the size and morphology in the synthesis of nanocrystals.[7] Since the superconducting phase of iron selenide, β-FeSe, is only stable below 457 °C[8], its synthesis requires two heating cycles and an annealing cycle[3,9] or a solvothermal synthesis as previously discussed.[6,10] Due to the presence of competing phases (β-FeSe, α-FeSe, Fe_7Se_8) β-FeSe provides a good system for use as a case study to investigate alternative synthetic techniques. We previously demonstrated the role of triphenylphosphine in promoting reactivity between $CuCl_2$ and Na_2Se_2 to form a metastable polymorph $CuSe_2$ in a metathesis reaction.[11] Triphenylphosphine also has a reasonable range at which it is

[a] Department of Chemistry, Colorado State University, Fort Collins, Colorado 80523-1872, United States. Tel: 970-491-2958; E-mail: James.Neilson@colostate.edu
[b] Advanced Photon Source, Argonne National Laboratory, Argonne, Illinois 60439-4858, United States.

† Electronic Supplementary Information (ESI) available: [details of any supplementary information available should be included here]. See DOI: 00.0000/00000000.

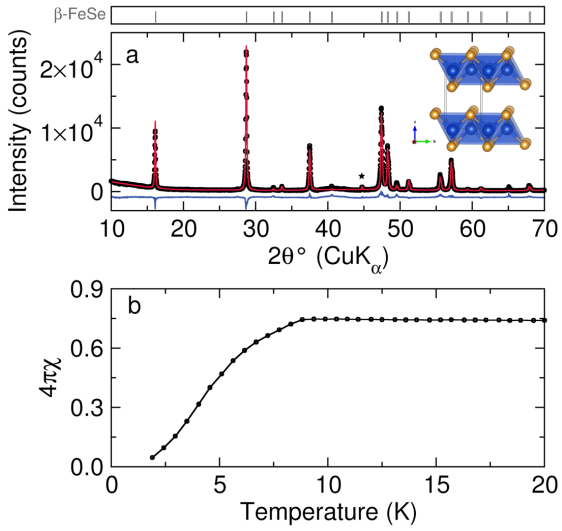

Fig. 1 (a) PXRD of the products of the iron selenide reactions completed with triphenylphosphine. A Rietveld refinement modeling 99% β-FeSe and 1% Fe (starred peak) is shown in red with the difference curve in blue. The structure of β-FeSe with iron (blue) and selenium (gold) is shown to the right. (b) Temperature versus $4\pi\chi$ of iron selenide prepared using a triphenylphosphine flux measured with the MPMS.

molten and stable making it suitable for reactions at elevated temperatures suitable for producing extended solids (T_m = 80 °C, T_{decomp} > 400 °C). The formation of β-FeSe is confirmed by powder X-ray diffraction (PXRD) and magnetism measurements. Control reactions without a flux and with non-Lewis basic fluxes demonstrate the necessity of a molten and reactive flux. Nuclear magnetic resonance (NMR) and *in situ* X-ray diffraction (XRD) and pair distribution function (PDF) analysis suggest that the formation of an adduct between the selenium and triphenylphosphine promotes mass transport between the iron and the selenium while also serving to decrease the chemical potential of selenium. Overall, this research shows that triphenylphosphine fluxes can enable the synthesis of low-temperature phases of solid-state materials and may aid in the discovery of new functional materials.

Experimental

Purified iron powder (NOAH Technologies Corporation, 99.9%), selenium shot (Alfa Aesar, 99.999%) or powder (Sigma Aldrich, 99.5%), and triphenylphosphine flakes (Alfa Aesar, 99+%) in a 1:1:1.5 mole ratio were sealed in a fused SiO_2 ampoule (10 mm ID/12 mm OD) under vacuum ($p \leq 10$ mTorr). The ampoule was heated at a rate of 10 °C/min to 325 °C and dwelled for 117 h in a muffle furnace before quenching in water. Iron powder was purified of surface oxides by sealing it in in a fused SiO_2 ampoule under vacuum ($p \leq 10$ mTorr). The ampoule was heated at a rate of 10 °C/min to 980 °C and dwelled for 16 h before cooling in the furnace. The iron was transferred to a new evacuated ampoule and the heating cycle was repeated until the iron appeared shiny. Diffraction analysis with an internal standard reveals that the iron is ~75 wt% amorphous.

A series of exploratory reactions were completed by varying the reaction conditions as summarized in detail in the Supplemental Information†. For each reaction, purified iron powder, selenium shot, and triphenylphosphine flakes in the desired stoichiometric quantities were sealed under vacuum in a SiO_2 ampoule. The sealed ampoule was heated in a furnace at a ramp rate of 10 °C/min up to the final temperature for the desired reaction time. The "air-cooled" reactions were removed from the furnace and left at room temperature; quenched reactions were taken from the furnace and placed directly into a water bath. The reactions above 350 °C were sealed in 4 mm ID, 6 mm OD ampoules and were placed in metal piping (open both ends) to contain reactions in the event of gas formation (no ampoules failed). Several control reactions were completed: without flux, with eicosane (Acros Organics, 99%), and with triphenylamine (TCI America, 98%). Once the reactions were completed, the organic materials were mechanically removed with a steel spatula from each reaction and set aside for additional analysis. The remaining material was washed in ~10 mL benzene (EMD Millipore, 99%) per 500 mg FeSe and stirred until the residual flux dissolved. Samples for magnetic characterization were kept air-free once the reaction had completed. For these samples, the ampoules were opened in an argon-filled glove box and rinsed with degassed, dry benzene (deoxygenated over CaH_2 and distilled) in the glovebox. For all samples, once the triphenylphosphine dissolved, the samples were ground with a mortar and pestle for 2-3 min until homogenous.

Laboratory powder X-ray diffraction data were collected on a Bruker D8 Discover diffractometer with CuKα radiation and a Lynxeye XE-T position-sensitive detector. Samples were prepared on a zero-diffraction Si wafer. *Ex situ* total X-ray scattering data sets for pair distribution function (PDF) analysis were collected on a Panalytical Empyrean Diffractometer with the GaliPIX 2D detector using AgKα radiation. Samples were packed in 0.0395 in outer diameter kapton capillaries sealed with modeling clay.

The samples for *in situ* analysis were prepared for analysis by ball milling iron, selenium, and triphenylphosphine in a 1:1:0.5 mole ratio at T = 77 K using a Retsch cryomill. The samples were milled in a stainless steel jar with stainless steel ball bearings at 30 Hz for 15 min after cooling. Milling was performed to provide an intimate mixture and to facilitate capillary packing. The mixture was then packed in a 1.1 mm borosilicate capillary in air and immobilized with quartz wool and measured in a flow cell furnace[12] using the 11-ID-B beamline at the Advanced Photon Source at Argonne National Laboratory. Surface tension of the melt kept the contents within the capillary. No apparent oxidation products were observed over the course of the reaction. The reaction was heated up at 10 °C/min to 325 °C taking diffraction patterns every 25 °C from a distance of 1 m for XRD and 200 mm for PDF. A CeO_2 standard was also measured for sample-detector distance calibration. The wavelength was 0.2113 Å, a Q_{min} of 0.5 Å^{-1} and a Q_{max} of 5.95 Å^{-1} for XRD or a Q_{max} of 23 Å^{-1} for PDF was used during data transformation. GSAS-II was used to transform the raw data to PDF and PDFgui was used to analyze the data.[13,14]

A variety of compositions were picked throughout the phase space and are discussed specifically in the results. All of these re-

actions were completed following the heating schedule of heating at 10 °C/min up to 325 °C, dwelling for 72 h and slow-cooling for 45 h. After the reactions were completed, organic residue was mechanically separated for NMR spectroscopy experiments. The remaining product powder was ground and analyzed through PXRD. *Ex situ* PDF analysis as described above was completed on the product from the reaction 8Fe + Se + PPh_3 as well as the purified iron powder. This reaction was chosen for analysis due to the lack of iron in the products as observed by PXRD Rietveld refinement.

Magnetism measurements were completed with the Quantum Design Inc. Magnetic Properties Measurement System (MPMS-XL). Samples were prepared for the MPMS in the glovebox by weighing approximately 25 mg of the product into a gelatin capsule. Kapton was wrapped around the sample to keep it air-free. Upon removal from the glovebox, the sample was placed in a straw and loaded in the MPMS. The zero field-cooled magnetization was measured from 1.9 K to 20 K at a field strength of H = 5 Oe. The magnetization was converted to volume susceptability using field strength, mass, and theoretical density of ρ = 5.68 g/cm^3.[3]

Room temperature ^{1}H and ^{31}P NMR spectra were taken of the white organic residue of several reactions. Samples were prepared for NMR by placing approximately 10 mg of the nominal triphenylphosphine residue into an NMR tube and adding 700 μL of deuterated benzene (Cambridge Isotope Laboratory Inc., 99.5%). Samples were placed in an Agilent (Varian) 400 MHz NMR. Control room temperature ^{1}H and ^{31}P NMR spectra were also taken separately of the deuterated benzene solvent and a sample of the unreacted triphenylphosphine flakes prepared in the same way as the post-reaction specimens.

Results and Discussion

Superconducting iron selenide forms with a 1 Fe to 1 Se ratio in a 1.5 molar excess of triphenylphosphine flux at 325 °C after 117 h. PXRD confirms the crystalline purity with only 1 mole percent Fe detected (Figure 1a). Based on the onset of volume exclusion of a magnetic field, the superconducting transition temperature is around T_c = 8.9 K (Figure 1b), and is a gradual transition (in contrast to the sharp T_c = 8.5 K transition observed in the literature[3]). The T_c is extremely sensitive to the stoichiometry, $Fe_{1+\delta}Se$, with deviations from $Fe_{1.01}Se$ causing a decrease in the transition temperature.[3,9] The positive shift in the $4\pi\chi$ of the iron selenide synthesized using a triphenylphosphine flux compared to the $4\pi\chi$ reported in literature can be attributed to the slight iron excess in the sample. Based on the observed diamagnetic transition, the superconducting volume fraction is around 70% (Figure 1b), which was reproducible across multiple samples. The β-FeSe maintains the structure and properties as iron selenide synthesized without significant oxygen contamination or stoichiometric deviation.

To explore how triphenylphosphine impacts the reaction to form β-FeSe, control reactions with different organic molecules (NPh_3, $C_{20}H_{42}$) were completed. A summary of products from these control reactions is shown in Table S2. The reaction without a flux forms a mixture of Fe-Se phases along with Fe, consistent

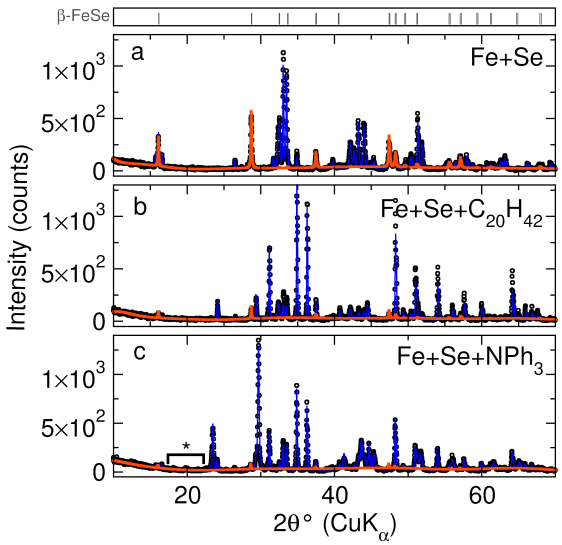

Fig. 2 PXRD of the products of the iron selenide reactions completed with (a) no flux, (b) eicosane, and (c) triphenylamine. The peaks barely visible above the background (marked by an asterix) are from residual PPh_3. Rietveld refinement modeling β-FeSe for each diffraction pattern is shown in orange and the fit for the remaining phases is shown in blue.

with a mass transport-limited reaction (Figure 2a; majority products: β-FeSe, Fe_3Se_4). Performing the reaction in molten eicosane wax ($C_{20}H_{42}$, a chemically unfunctionalized alkane) also forms a variety of products indicating that a molten and reactive flux is necessary for a complete reaction (Figure 2b; majority products: $FeSe_2$, β-FeSe, Fe_3Se_4). Reaction in molten triphenylamine also forms a distribution of products (Figure 2c; majority products: Se, $FeSe_2$). This suggests the Lewis basicity is an important factor for forming the desired product. This is further supported by the successful reaction of Ph_3PSe with iron to form β-FeSe with 96 mol% purity (impurities: 3 mol% α-FeSe, and 1 mol% Fe), indicating that the adduct is the reactive species (Figure S1). Together, these controls demonstrate the necessity of a molten and partially reactive flux, where reactivity is dictated by Lewis basicity.

A number of test reactions completed at higher and lower temperatures as well as shorter dwell times yielded impure products. Higher temperatures caused the flux to decompose while reactions completed at lower temperatures showed a mixture of α-FeSe and β-FeSe. Shorter reactions as well as reactions with shorter cool times also contained a mixture of α-FeSe and β-FeSe. Thus it was determined that the length of time at higher temperature is important for complete reaction to β-FeSe.

To gain more insight into the nature of reactivity, *in situ* XRD and PDF experiments were completed on a mixture of iron, selenium, and triphenylphosphine (Figure 3). Phase fractions determined through Rietveld refinements are shown in Figure S2. Based on Rietveld analysis of these data where triphenylphosphine selenide formation is observed, triphenylphosphine selenide forms immediately once triphenylphosphine begins to melt around 75 °C. The reaction goes through a phase where everything but the iron is molten, and once a temperature of 275 °C is

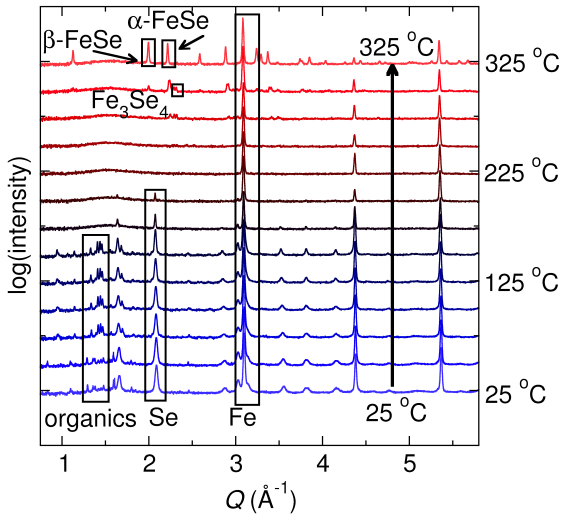

Fig. 3 Diffraction patterns of a 2Fe + 2Se + PPh_3 reaction collected *in situ* upon heating with each temperature offset for clarity in 25 °C increments. The most intense peak for each phase is labeled; note the logarithmic intensity axis.

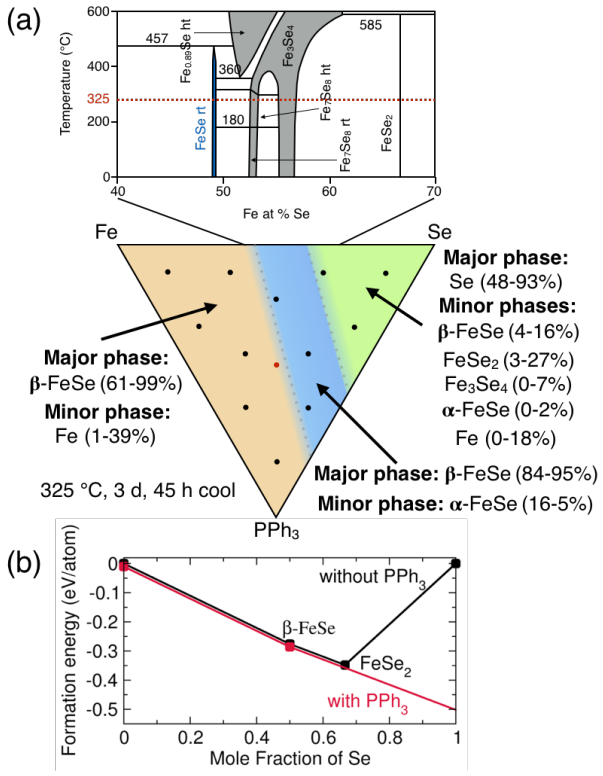

Fig. 4 (a)Ternary phase map between iron, selenium, and triphenylphosphine. The binary iron selenide phase diagram is shown above. The dots on the ternary phase map represent completed reactions; the red dot is the optimized reaction. (b) Formation energies (T = 0 K, DFT)[15] of computed and stable Fe-Se species that form the convex hull without triphenylphosphine (black line) in contrast to the offset line showing the extrapolated effective chemical potential of selenium (as to avoid $FeSe_2$ formation) in the presence of excess triphenylphosphine (red line).

reached, iron selenide begins to form. Initially, α-FeSe and Fe_3Se_4 form and these phases disappear as β-FeSe forms at higher temperatures. It has been suggested that less stable products often form first (e.g., Ostwald's step rule) which explains the formation of these iron selenide phases initially over the expected FeSe product.[16] At 325 °C both α-FeSe and β-FeSe are present indicating that β-FeSe is stabilized through dwelling at the reaction temperature. Incomplete conversion to β-FeSe is observed *in situ* since the reaction was not kept at temperature for an extended period of time. This supports the *ex situ* observation that a long reaction time (∼117 h) is required for "complete reaction". *In situ* PDF of the reaction between iron, selenium, and triphenylphosphine as well as the reaction between triphenylphosphine and selenium (Figure 5) support what is observed in the *in situ* XRD with how the reaction progresses. Additionally the *in situ* PDF analysis shows no indication of large amounts of amorphous materials, as assessed from analysis of the stoichiometry. There is the possibility for small amounts of amorphous phases making up less than 2.5 mol% of the phases present.[17]

Exploring the ternary phase space demonstrated that the reaction does not follow an extension of the Fe-Se phase diagram. A map of the ternary phase space between iron, selenium and triphenylphosphine is shown in Figure 4a. β-FeSe exists as the predominate phase for $\leq$ 50 mol% Se while other phases are present depending on the ratio of the reactants (Table S2); selenium is the primary phase for $\geq$ 50 mol% Se. This indicates that reaction in a triphenylphosphine flux preferentially forms β-FeSe. The selenium-rich reactions yield more than three phases, suggesting that the phase map does not represent a true equilibrium, as based on Gibbs' phase rule. Based on the phase fractions calculated from Rietveld refinements in relation to the starting composition, the reaction products are deficient in crystalline iron. PDF analysis of the starting iron as well as a completed reaction indicate a significant fraction of diffraction amorphous iron (e.g. nanocrystalline) present in the precursor, which accounts for the iron missing from analysis of the diffraction data (Figures S3, S4). NMR spectroscopy performed on the post-reaction organic residue samples from these completed reactions reveal signals consistent with triphenylphosphine and triphenylphosphine selenide (Figure 6).[18] Reactions completed with excess selenium contained mostly triphenylphosphine selenide, while reactions completed with excess iron contained mostly triphenylphosphine.

The results of these reactions suggest that triphenylphosphine does not just provide a liquid medium for accelerated mass transport, but that triphenylphosphine also reduces the reactivity of selenium. It appears that in reactions containing more triphenylphosphine the product $FeSe_2$ is avoided, which suggests that the chemical potential of selenium is reduced. This is shown schematically in Figure 4b using calculated formation energies for the reportedly stable Fe-Se phases from the Materials Project (Table S3).[15] Extrapolation of the T = 0 K calculations suggests that the triphenylphosphine reduces the effective chemical potential by at least 0.5 eV/atom. Chemically this is rationalized by the stability of the dative bond in the Se-PPh_3 adduct, thus reducing the reactivity of the selenium towards iron. This notion of a partially reactive flux provides a handle for designing selective reactions.

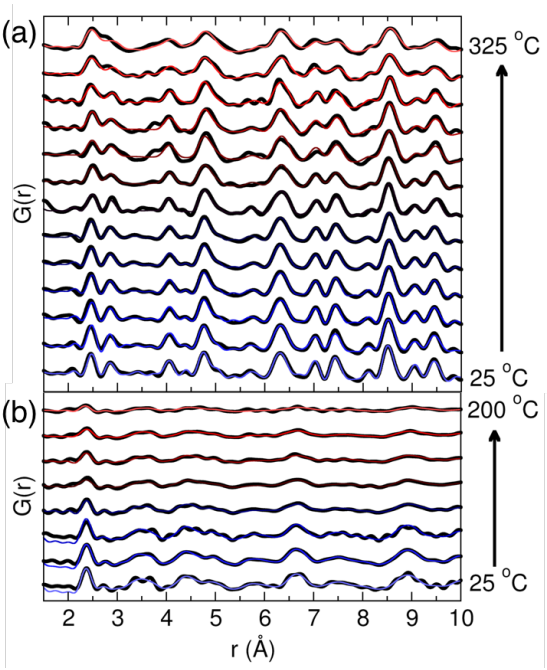

Fig. 5 PDF analysis of total scattering data collected *in situ* from the reactions of (a) iron and selenium in a triphenylphosphine flux and (b) selenium and triphenylphosphine upon heating. Data shown in black and fits shown in color gradient from blue to red upon heating.

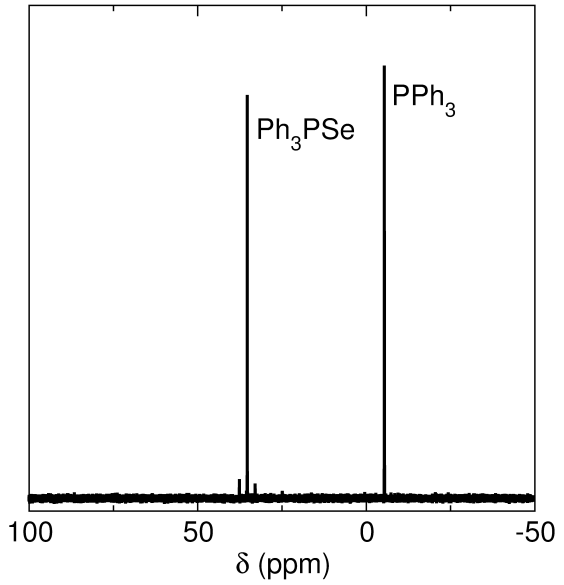

Fig. 6 ^{31}P NMR spectrum of the triphenylphosphine flux from the iron selenide reaction completed at 325 °C for 24 h with a 30 h cool.

Triphenylphosphine acts as a low-temperature, molten flux for materials synthesis as exemplified with β-FeSe. The optimized β-FeSe synthesis reacts the elements in a triphenylphosphine flux at 325 °C for 117 h. *In situ* analysis of the iron selenide reaction shows formation of a Se-PPh_3 adduct that reduces the chemical potential of Se in its reaction towards iron, while also forming a high mobility, liquid phase. This synthetic approach has the potential to improve the syntheses for many solid-state materials at lower temperatures and with chemical selectivity.

Acknowledgments

This work was supported by the National Science Foundation (DMR-1653863). JRN acknowledges partial support from a Sloan Research Fellowship and a Cottrell Scholar Award. This research used resources of the Advanced Photon Source, a U.S. Department of Energy (DOE) Office of Science User Facility operated for the DOE Office of Science by Argonne National Laboratory under Contract No. DE-AC02-06CH11357.

Conflicts of interest

There are no conflicts to declare

Notes and references

1 A. Stein, S. W. Keller and T. E. Mallouk, *Science*, 1993, **259**, 1558–1564.
2 T. A. Bither, R. J. Bouchard, W. H. Cloud, P. C. Dokohue and W. J. Siemons, *Inorg. Chem.*, 1968, **59**, 2208–2220.
3 T. M. McQueen, Q. Huang, V. Ksenofontov, C. Felser, Q. Xu, H. Zandbergen, Y. S. Hor, J. Allred, A. J. Williams, D. Qu, J. Checkelsky, N. P. Ong and R. J. Cava, *Phys. Rev. B*, 2009, **79**, 014522.
4 M. G. Kanatzidis, R. Pottgen and W. Jeitschko, *Angew. Chem. Int. Ed.*, 2005, **44**, 6996–7023.
5 S. B. Zhang, Y. P. Sun, X. D. Zhu, X. B. Zhu, B. S. Wang, G. Li, H. C. Lei, X. Luo, Z. R. Yang, W. H. Song and J. M. Dai, *Supercond. Sci. Technol.*, 2009, **22**, 0–4.
6 J. T. Greenfield, S. Kamali, K. Lee and K. Kovnir, *Chem. Mater.*, 2015, **27**, 588–596.
7 T. P. A. Ruberu, H. R. Albright, B. Callis, B. Ward, J. Cisneros, H.-j. Fan and J. Vela, *ACS Nano*, 2012, **6**, 5348–5359.
8 H. Okamoto, *J. Phase Equilib.*, 1991, **12**, 383–389.
9 F.-C. Hsu, J.-Y. Luo, K.-W. Yeh, T.-K. Chen, T.-W. Huang, P. M. Wu, Y.-C. Lee, Y.-L. Huang, Y.-Y. Chu, D.-C. Yan and M.-K. Wu, *Proc. Natl. Acad. Sci.*, 2008, **105**, 14262–14264.
10 F. Nitsche, T. Goltz, H.-H. Klauss, A. Isaeva, U. Muller, W. Schnelle, P. Simon, T. Doert and M. Ruck, *Inorg. Chem.*, 2012, **51**, 7370–7376.
11 A. J. Martinolich, R. F. Higgins, M. P. Shores and J. R. Neilson, *Chem. of Mater.*, 2016, **28**, 1854–1860.
12 P. J. Chupas, K. W. Chapman, C. Kurtz, J. C. Hanson, P. L. Lee and C. P. Grey, *J. of Appl. Crystallogr.*, 2008, **41**, 822–824.
13 B. H. Toby and R. B. Von Dreele, *J. Appl. Crystallogr.*, 2013, **46**, 544–549.
14 C. L. Farrow, P. Juhas, J. W. Liu, D. Bryndin, E. S. Božin, J. Bloch, T. Proffen and S. J. L. Billinge, *J. Phys.: Condens. Matter*, 2007, **19**, 335219.
15 A. Jain, S. P. Ong, G. Hautier, W. Chen, W. D. Richards, S. Dacek, S. Cholia, D. Gunter, D. Skinner, G. Ceder and K. a. Persson, *Appl. Phys. Lett. Mater.*, 2013, **1**, 011002.
16 A. Navrotsky, *Proc. Natl. Acad. Sci.*, 2004, **101**, 12096–12101.
17 J. Peterson, J. TenCate, T. Proffen, T. Darling, H. Nakotte and K. Page, *J. Appl. Crystallogr.*, 2013, **46**, 332–336.
18 G. Grossmann, M. J. Potrzebowski, U. Fleischer, K. Krüger, O. L. Malkina and W. Ciesielski, *Solid State Nucl. Mag. Res.*, 1998, **13**, 71–85.